SUPPORTING INFORMATION

S1. Distribution of the temperature sensors in the laboratory scale gully pot

This section describes the locations of the 23 DS18B20 temperature sensors installed in the 1:1 scaled gully pot model for the experimental campaign. Figure S1 shows the distribution of 18 sensors inside the gully pot; 4 sensors were installed at the bottom (one of them at the corner), and 2 sensors at heights of 50, 100, 150, 200, 250, 300, and ~500 mm, respectively. Temperature sensors were attached to the bottom and walls by using adhesive square backings and tie wraps. In addition, 4 additional sensors were installed to measure the temperature at the gully pot inlet, in the outer tank, in the 550-L water tank, and the room temperature.

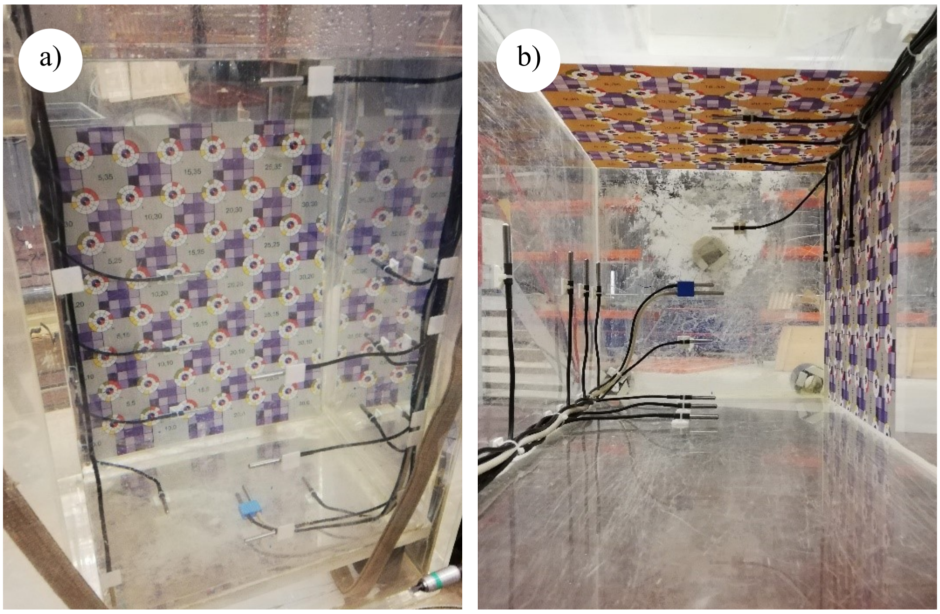

Figure S1. *Lateral (a) and top (b) view photographs of the temperature sensor distribution inside the gully pot model.*

S2. Reference sediment depths with the SfM technique

The Structure from Motion (SfM) technique was selected to perform high precision measurements of the sediment depths inside the gully pot model during the experimental campaign. Submerged images were taken to reconstruct the sediment surface by introducing a GoPro HERO 9 Black camera (GoPro, USA) in the standing water layer (Figure S2a). An average of 25 images were taken to perform the 3D reconstruction with the SfM technique, setting an image overlapping of 60% by following previous references.[1,2] The 3DF Zephyr Free and MeshLab software were used to perform the reconstruction and the scaling and referring the 3D model of the sediment surface (Figure S2b). The average depth of the 3D surface model was considered as the reference sediment depth. This technique was only applied for sand beds because organic and mixture sediments led to a high turbidity in the standing water layer due to the fine fractions. For the latter sediment types, measuring tapes were used to perform visual observations of the sediment depth.

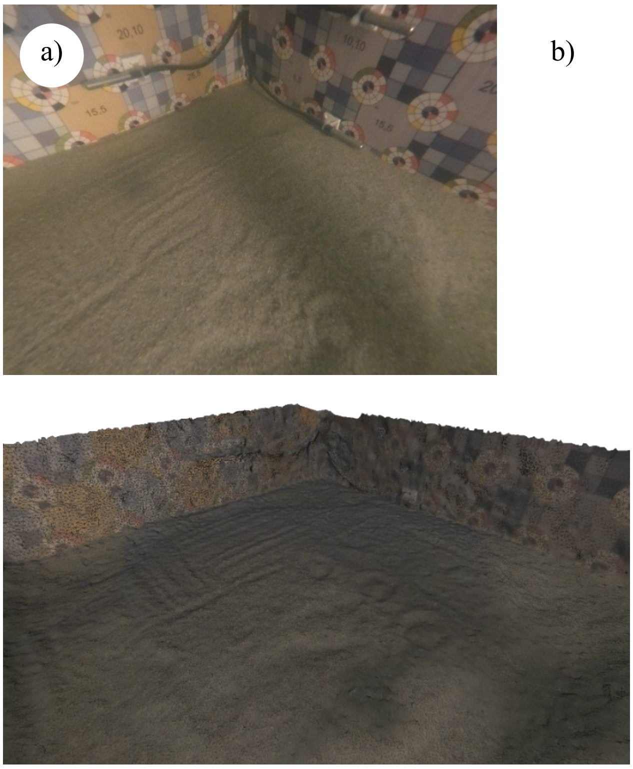

Figure S2. *Raw image (a) and 3D model reconstruction (b) of the sand bed. Source: Regueiro-Picallo et al.*[3]

S3. PMMA-acrylic thermal properties

The heat loss at the walls and the bottom of the gully pot was defined by a Cauchy-type boundary condition in the 2D heat diffusion model. The acrylic PMMA influences the convective heat transfer coefficient, which can be expressed as $h = k_{tPMMA}/e$, where k_{tPMMA} is the thermal conductivity of the PMMA, which can be ranged between 0.15-0.25 W/m/ºC,[4] and e is the thickness of the gully pot wall (e = 18 mm). For this purpose, the h-value was estimated from the fit of the experimental and simulated temperature series in the sediment layer for those experiments with negative gradients, i.e., ΔT1 and ΔT2. The simulated sediment temperatures were computed with the 2D heat diffusion model by considering the measured sediment depths and thermal properties. A fitting model was programmed in MATLAB by establishing the minimum value of the root mean square error (RMSE) between the experimental and simulated sediment-bed temperatures as the objective function. Figure S3 shows the best-fitting h-values for each experiment with a significant oscillation between 9.0 and 16.0 W/m^2/ºC. As a result, the convective heat transfer coefficient showed a median value of h = 12.8 W/m²/ºC and, consequently, k_{tPMMA} = 0.23 W/m/ºC, similar to the reference range.

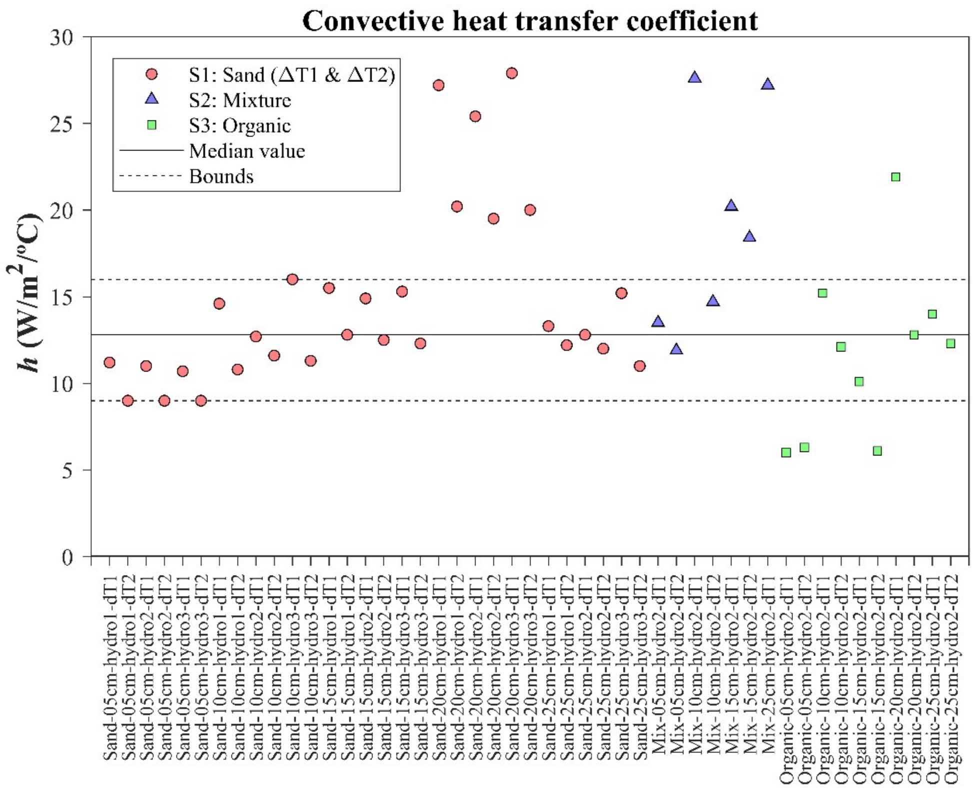

Figure S3. *Convective heat transfer coefficients (h) that showed the best fit between the experimental and simulated sediment-bed temperatures.*

S4. Water temperature gradient statistics from field measurements

Field temperature measurements were recorded in the standing water layer of two gully pots during a period of 3 months, between July and September 2022, to design the temperature gradients introduced in the lab-scale experimental campaign. lab-scale model. Temperature data are openly accessible, including information on the location of the gully pots and the configuration of the measuring devices.[3] Rainfall data is also accessible from the Met Office Observations Network.[5] Table S1 summarises the events observed for each gully pot (GP1 and GP2) for which rainfall accumulation exceeded 1.5 mm in a one-hour period and, consequently, a temperature gradient was observed in the standing water layer, which was calculated as the difference between the initial and the maximum or minimum temperature during the event (positive and negative gradients, respectively). Additional information regarding the antecedent dry weather period, the maximum rainfall intensity, the rainfall duration and the average air temperature is also provided.

Table S1. *Summary of the rainfall-runoff events with a rainfall accumulation higher than 1.5 mm during the field campaign: Datetime format of the rainfall start, antecedent dry weather period (days), rainfall accumulation (mm), maximum rainfall intensity (mm/h), rainfall duration (hours), average air temperature (ºC), and temperature gradients in GP1 and GP2 (ºC).*

Datetime. UTC (dd/mm/yyyy HH:MM)	Antecedent dry weather period (days)	Rainfall accumulation (mm)	Max. rainfall intensity (mm/h)	Rainfall duration (hours)	Avg. air temperature (ºC)	Temperature gradient GP1 (ºC)	Temperature gradient GP2 (ºC)
21/07/2022 06:12	14	6.5	7.2	2.0	17.6	(-)	-2.4
15/08/2022 17:03	25	27.0	135.6	0.5	19.4	-7.0	-6.4
17/08/2022 07:20	2	14.9	30.6	1.9	19.2	-3.1	-2.7
05/09/2022 18:41	19	13.9	19.8	3.5	18.0	-0.4	+1.7
06/09/2022 20:35	1	29.9	87.0	3.5	17.9	-4.0	-3.1
08/09/2022 05:06	1	1.9	6.0	0.5	16.2	(-)	-1.7
09/09/2022 09:49	1	2.4	6.6	0.5	16.0	(-)	-0.6
09/09/2022 13:34	0	6.9	33.6	0.4	16.3	-3.4	-1.2
09/09/2022 18:01	0	5.1	24.6	0.7	15.7	-2.6	-1.6
09/09/2022 21:19	0	5.5	13.8	1.7	15.6	-2.6	-0.5
10/09/2022 01:03	0	2.8	4.8	1.5	15.5	-0.6	(-)
16/09/2022 01:19	6	2.5	13.2	0.3	13.1	-4.3	-4.4
16/09/2022 07:12	0	2.1	10.8	0.3	11.8	-1.3	-1.5
16/09/2022 12:56	0	1.8	6.6	1.3	13.2	-0.7	+1.1
16/09/2022 22:07	0	2.4	6.0	0.8	11.5	-2.2	-2.4
17/09/2022 00:37	0	3.2	10.8	0.6	11.2	-5.2	-0.8
17/09/2022 05:25	0	1.8	6.0	0.7	10.6	-1.8	+1.3
17/09/2022 15:55	0	2.8	7.8	1.3	12.0	-1.1	+0.5
18/09/2022 07:41	0	2.0	12.0	0.1	12.8	-3.1	+1.4
18/09/2022 11:04	0	2.8	10.2	0.5	12.5	-3.3	+0.4

(-) no observation data.

S5. Water temperature stratification in the lab-scale experiments

The water layer was conditioned by the outlet pipe of the gully pot model and the sediment layer, i.e., low sediment depths such as h_{sed} = 50 mm led to large water layers. Under these conditions, temperature stratification in the water layer may appear because of the temperatures at the room (top boundary), the outer tank (lateral boundaries) and the sediment (bottom boundary). For this purpose, temperature time series of sensors located in the water layer were analysed. The median absolute deviation ($MAD = median(|T_i - \overline{T}|)$, where T is the temperature time series and i refers to each sensor submerged in the water layer) of the temperature time series was used as a reference to show temperature homogeneity in the water layer (Figure S4). Overall, no significant deviations in the water layer temperatures were observed during the experiments as the maximum MAD-values were below 0.35 ºC.

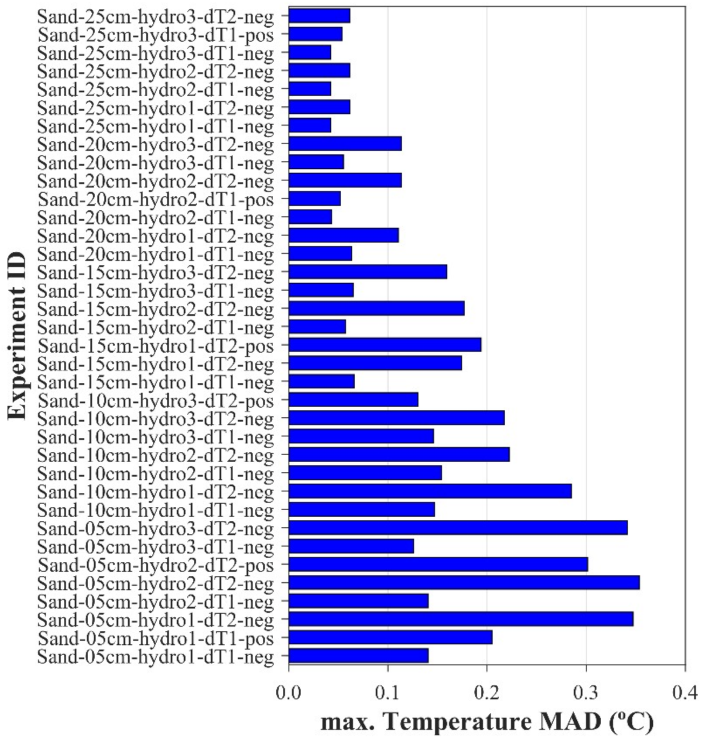

Figure S4. *Maximum MAD-values of the temperature time series measured in the standing water layer of the gully pot model.*

S6. Measured and simulated temperatures in the sediment layer

The sediment depth estimation in the gully pot model was carried out by comparing measured and simulated temperatures in the sediment layer, using the sensors closest to the water-sediment interface as a reference. This process was iterative by simulating sediment depth conditions to find the depth that minimised the error between the experimental and numerical temperature time series. Figure S5 shows three examples of the experimental-numerical comparison of sediment temperatures for a sediment depth of 50 mm, temperature gradient ΔT2, $Hydro_2$ flow conditions, and the three types of sediments, resulting in a Root Mean Square Error (RMSE) between the time series of 0.08 ºC for the sand (Figure S5, a), 0.10 ºC for the mixture (Figure S5, b), and 0.12 ºC for the organic sediment (Figure S5, c), respectively.

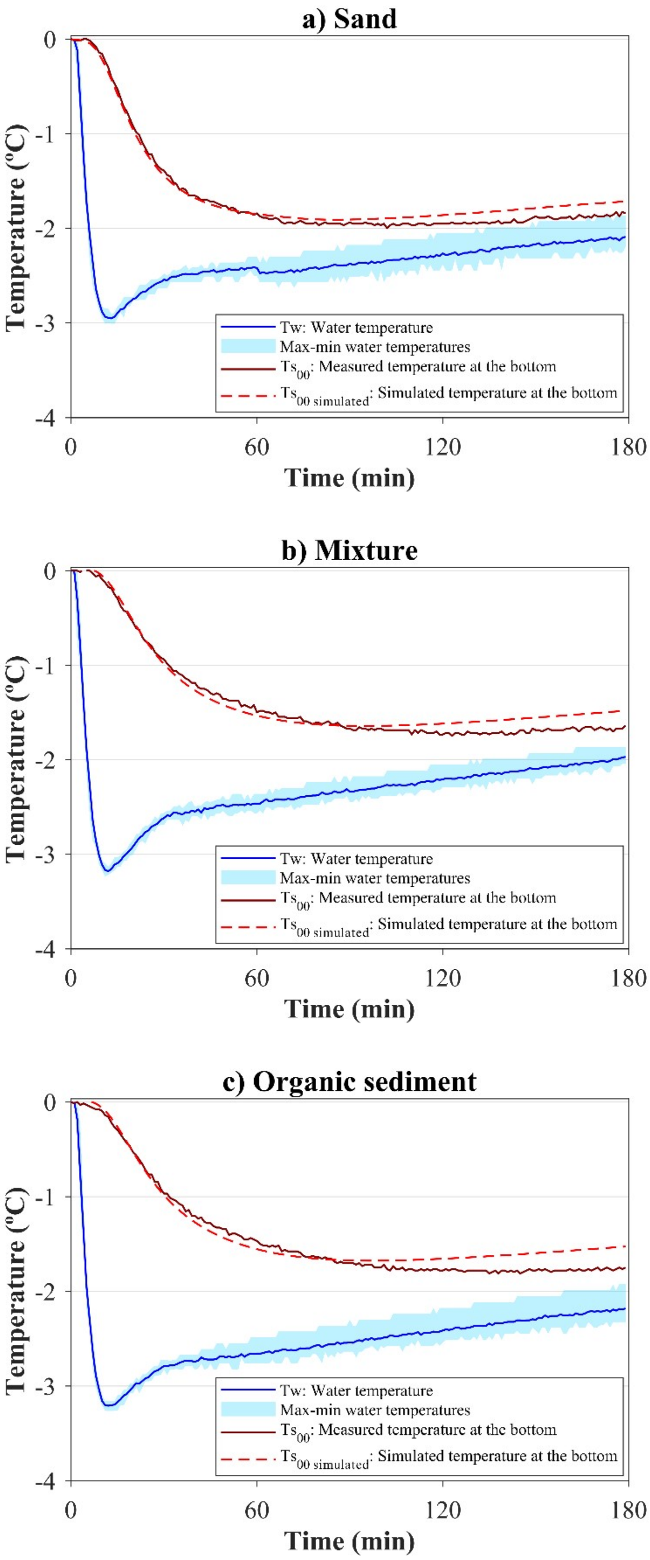

Figure S5. *Experimental and numerical sediment temperature time series for test conditions with a sediment height of* h_{sed} *= 50 mm, temperature gradient* $\Delta T2$*,* $Hydro_2$ *flow conditions, and three sediment types: sand (a), mixture (b), and organic (c). Water temperature (blue line) represents the average of the experimental measurements (light blue area), which was used as top-boundary input of the 2D heat diffusion model. Note that temperatures are shown relative to the initial measurements.*

S7. Comparison between 2D and 3D heat diffusion models

The temperature sensors were installed on the central axis of the gully pot walls. Although sensors were installed on all four walls, symmetry can be assumed due to the squared section of the gully pot model. Therefore, each sensor was mainly influenced by one boundary, resulting in 175 mm distance (half the length of the scupper) from the adjacent boundary. Temperatures in the sediment layer were simulated where the sensors selected to estimate sediment depths were located with the aim of quantifying the differences between the 2D and 3D models. The maximum MAD-values of the simulated temperature time series with the 2D and 3D model were below 0.05 ºC, with lower deviations for the experiments performed with organic sediments (< 0.03 ºC). In addition, sediment depth estimations were compared using the 2D and 3D models and experiments with sands and ΔT1 and ΔT3 temperature gradients, obtaining maximum absolute deviations of 2 mm. In all cases, the 2D model overestimated the sediment depth, thus being conservative.

Furthermore, the influence of the gully pot geometry on the simulation of temperatures in the sediment layer was studied. For this purpose, different gully pot lengths, ranged from 50 mm to 700 mm (2 times the width of the gully pot model) were simulated with the 3D model, considering a constant width (Figure S6a). Figure S6b shows the relationship between the temperature deviations simulated with the 2D and 3D models and the gully pot length for a test condition with h_{sed} = 150 mm, inorganic-sand sediment, $Hydro_2$, and temperature gradient ΔT1.

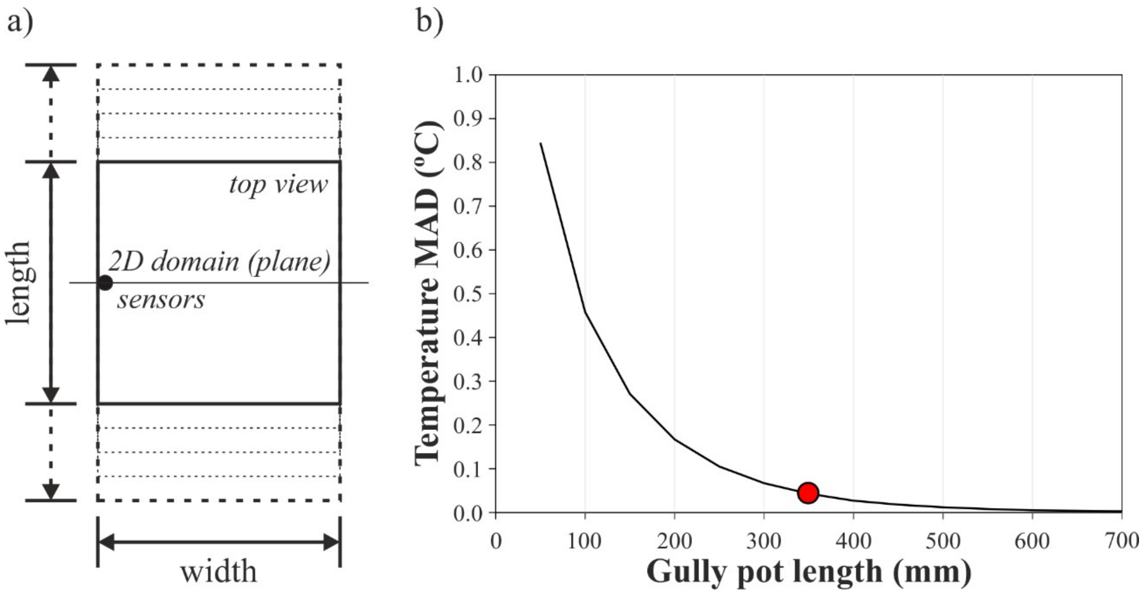

Figure S6. *Gully pot length range for simulating sediment temperatures with the 3D heat diffusion model (a), and relationship between the gully pot length and the temperature MAD-values, obtained from the temperatures in the sediment layer simulated with the 2D and 3D models.*

S8. References

1. J. A. Morgan, D. J. Brogan and P. A. Nelson, Application of Structure-from-Motion photogrammetry in laboratory flumes, *Geomorphology*, 2017, 276, 125-143. https://doi.org/10.1016/j.geomorph.2016.10.021
2. J. Naves, J. Anta, J. Puertas, M. Regueiro-Picallo and J. Suárez, Using a 2D shallow water model to assess Large-Scale Particle Image Velocimetry (LSPIV) and Structure from Motion (SfM) techniques in a street-scale urban drainage physical model. *J. Hydrol.*, 2019, 575, 54-65. https://doi.org/10.1016/j.jhydrol.2019.05.003
3. M. Regueiro-Picallo, A. Moreno-Rodenas and F. Clemens-Meyer, *Measuring sediment deposits in gully pots from temperature signals*, ZENODO, 2023. https://doi.org/10.5281/zenodo.10226224
4. Omnexus: The material selection platform. Thermal conductivity, https://omnexus.specialchem.com/polymer-property/thermal-insulation, (accessed 2 April 2024).
5. The UK Met Office Weather Observation Website (WOW), https://wow.metoffice.gov.uk/observations/details/20230130qobp94fyiwe65gsryyb96smpma, (accessed 20 February 2023).